JOURNAL OF MATERIALS SCIENCE 32 (1997) 3123–3128

# Characterization of cathodically deposited carbonaceous films on a silicon substrate

S. E. KWIATEK*, V. DESAI
*Department of Mechanical and Aerospace Engineering, University of Central Florida, Orlando, FL 32816, USA*

P. J. MORAN
** Mechanical Engineering Department, United States Naval Academy, Annapolis, MD 21402, USA*

P. M. NATISHAN
*Naval Research Laboratory, Washington, DC 20375, USA*

Carbon-based deposits were electrochemically formed on silicon substrates in ethanol at room temperature. This work was based on the work reported by Namba, who described the electrochemical deposition of diamond from organic solutions. The deposits were analysed using a scanning electron microscope, energy dispersive spectroscopy (EDS), X-ray photoelectron spectroscopy (XPS), Raman spectroscopy and electrochemical impedance spectroscopy. Scanning electron micrographs showed some crystalline deposits on the silicon. EDS was unable to identify carbon in the film, but did reveal impurities such as sodium, potassium, calcium and zinc. It was later established that the impurities most likely came from impurities in the graphite used for a counter electrode. XPS showed the presence of carbon species, and subsequently Raman spectroscopy was used to classify further the carbon deposits. Raman spectroscopy showed the presence of amorphous carbon in some films, but no diamond peak was observed for any of the films. EIS revealed that the impedance of the deposited films was nearly identical to that of the uncoated silicon, and did not resemble the impedance of diamond. Thus, in this work, carbon–based films were formed electrochemically, but these films were not diamond.

## 1. Introduction

In recent years, several attempts have been made to electrochemically deposit diamond or diamond-like carbon films. Most notably, in 1992, Namba [1] reported the deposition of diamond-phase carbon films on a silicon substrate at low temperatures using an organic solution of ethyl alcohol. Electrodeposition of carbon films in an ethylene–glycol solution, and carbon fibres in a solution of carbon tetrachloride in an organic solution, have been reported [2, 3]. Because the electrodeposition takes place near room temperature, it greatly increases the number of substrates that can be used. Chemical vapour deposition (CVD), which is the most common method of diamond film deposition, must be done at temperatures greater than 800 °C [4]. Therefore, only substrates with high melting temperatures can be used. Depositing the films at low temperatures also minimizes the thermal stresses that can develop in both the films and the substrate as they cool.

This work examined the nature of carbon films formed using Namba's experimental procedures [1], and further investigated the feasibility of electrochemically depositing diamond films. Further characterization of the deposited films, including the evaluation of electrical and mechanical properties, has also been investigated. In this study, temperature was increased in an effort to improve deposition rates. Alternate methods of depositing diamond films in an organic solution were also examined.

## 2. Experimental procedure

A schematic diagram of the experimental apparatus is shown in Fig. 1. A flat specimen holder was used to create the electrochemical cell. This holder places a flat, circular specimen in physical contact with the electrolyte and in electrical contact (by means of a metal rod) with the power supply. A boron-doped P-type silicon material with 1 0 0 orientation was used as the substrate. The specimen was circular with an area of 0.493 $mm^2$ and a thickness ranging from 475–575μm. A graphite rod, a platinum wire and a palladium wire were all used at various times as counter electrodes for individual experiments.The electrolyte was approximately 850 ml denatured ethyl alcohol for the first four experiments and a 100% pure ethyl alcohol for the remaining experiments. The distance between the anode and cathode was approximately 3.8 cm. Voltages varied from 1250–1850 V and

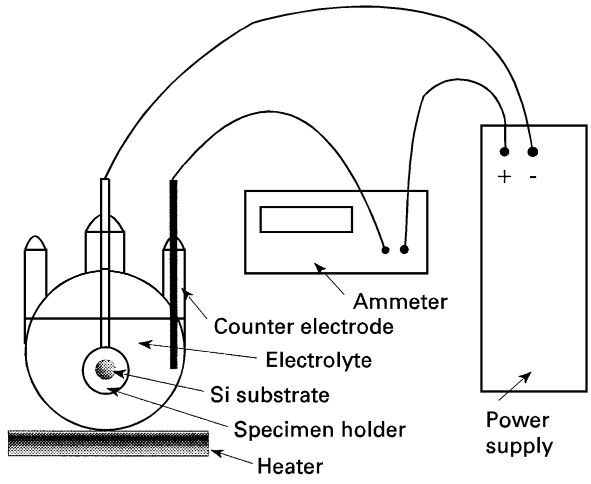

*Figure 1* Schematic diagram of experimental apparatus to deposit carbon films cathodically on a silicon substrate.

currents ranged from 0.5–0.9 mA. Temperature was varied from 20–52 °C, depending on the particular run. The sample was driven cathodically in all tests. Table I shows the experimental details of each experiment.

Specimens were prepared by rinsing with tap water, distilled water and the denatured ethanol. After rinsing all pieces separately, the substrate was placed in the specimen holder, rinsed with distilled water and ethanol, and immediately placed in the electrolyte. Deposition times varied in length from 20–140.5 h. After the samples were removed from the solution they were allowed to air dry before they were placed in the SEM. The time between removal from solution and SEM examination ranged from 5 min to 1 day.

The surfaces of selected samples were characterized using X-ray photoelectron spectroscopy. The escape depth for photoelectrons is of the order of nanometres so that X-ray photoelectron spectroscopy (XPS) was used to analyse the near-surface region. XPS measurements were made using a monochromatic. $\mathrm{AlK}_\alpha$ X-ray source (X-ray energy was 1446.6 eV). The spot size was 600 μm, the pass energy was 50 eV, and the base pressure was $8 \times 10^{-9}$ torr (1 torr = 133.322 Pa) or lower.

Deposits were also examined using a scanning electron microscope (SEM) and X-ray microanalysis. Selected samples were analysed by Raman spectroscopy performed in air and at room temperature. The samples were illuminated by directing radiation from an $\mathrm{Ar}^+$ ion laser emitting 40 mW at 514.6 nm, through a microscope and on to the sample surface. The inelastically scattered light was dispersed in a Spex Triplemate triple-pass monochromator where its intensity was measured with a liquid-nitrogen cooled CCD array. Electrochemical impedance spectroscopy (EIS) was also used to investigate the electrical properties of the deposited films on two samples.

## 3. Results and discussion

Scanning electron microscopy detected deposits on every sample, although the appearance of the deposit varied. The most common morphologies are shown in Figs 2 and 3. The deposits either appeared granular or showed a crystalline pattern. The thickness of the deposits varied over the entire surface of the sample.

Energy dispersive spectroscopy was also used to analyse all samples. Energy dispersive spectroscopy (EDS) detected unexpected elements such as calcium, zinc, potassium and sodium in several deposits. It was also noted that during the second test, the ethanol changed colour to a pale yellow and the current increased during the deposition process. It is thought that the high driving voltage caused the ethanol to break down, and impurities in the ethanol were deposited on the sample. Therefore, a 200 proof, 100% pure ethanol was used in all remaining tests to prevent any impurities from being deposited.

TABLE I Parameters of the experiments

| Sample | Counter electrode | Ethanol | Temperature | | Voltage (V) | Current (mA) | Time (h) |
|---|---|---|---|---|---|---|---|
| | | | (°F) | (°C) | | | |
| 1 | Graphite | Denatured | 68 | 20 | 1250 | 0.5–0.355 | 69 |
| 2 | Graphite | Denatured | 68 | 20 | 1750 | 0.5–1.26 | 138.5 |
| 3 | Graphite | Denatured | 68 | 20 | 1850 | 0.5–0.292 | 140.5 |
| 4 | Pd | Denatured | 68 | 20 | 610 | 0.5–0.281 | 193 |
| 5 | Pd | 200 proof | 120 | 49 | 2000 | 0.29–0.19 | 65 |
| 6 | Graphite | 200 proof | 112 | 44 | 2000 | 0.15–0.175 | 49.5 |
| 7 | Graphite | 200 proof | 112 | 44 | 1000 | 0.085–0.065 | 27 |
| 8 | Pt | 200 proof | 116 | 47 | 1220 | 0.091–0.178 | 114 |
| 9 | Graphite | 200 proof | 68 | 20 | 1000 | 0.115–0.098 | 72 |
| 10 | Graphite | 200 proof | 68 | 20 | 1000 | 0.080–0.033 | 94 |
| 11 | Graphite | 200 proof | 68 | 20 | 1000 | 0.120–0.074 | 95 |
| 12 | Graphite | 200 proof | 68 | 20 | 1000 | 0.096–0.076 | 50 |
| 13 | Graphite | 200 proof | 68 | 20 | 1000 | 0.076–0.034 | 115.5 |
| 14 | Graphite | 200 proof | 68 | 20 | 1000 | 0.084–0.055 | 49 |
| 15 | Graphite | 200 proof | 126 | 52 | 1000 | 0.081–0.072 | 20 |
| 16 | New Graphite | 200 proof | 68 | 20 | 1000 | 0.080–0.114 | 117.5 |
| 17 | Graphite | 200 proof | 68 | 20 | 1000 | 0.076–0.035 | 137.5 |
| 18 | Graphite | 200 proof | 68 | 20 | 1000 | 0.075–0.060 | 24 |
| 19 | Graphite | 200 proof | 68 | 20 | 1000 | 0.115–0.060 | 50.5 |

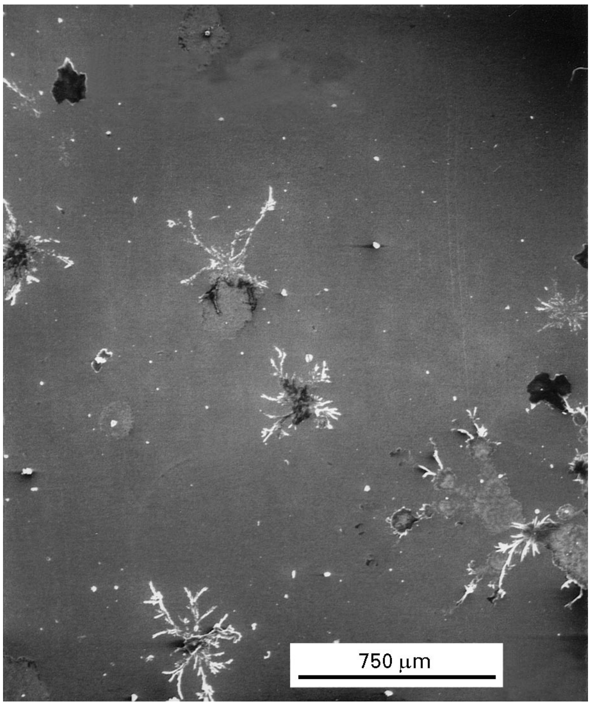

*Figure 2* Scanning electron micrograph of sample 12. The sample was run at 1000 V for 50 h in 200 proof ethanol at room temperature. The graphite counter electrode had been used in the 11 previous runs. The micrograph shows both granular and crystalline deposits.

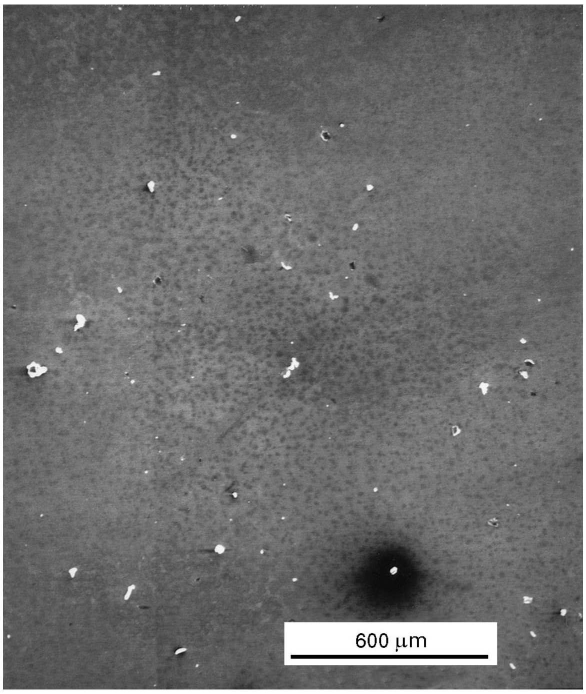

*Figure 3* Scanning electron micrograph of sample 16. Sample was run at 1000 V for 117.5 h in 200 proof ethanol at room temperature. This test utilized a new graphite counter electrode. The micrograph shows a granular deposit only.

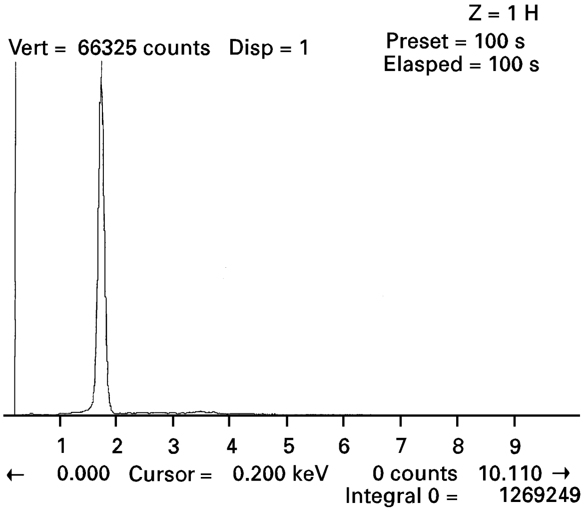

*Figure 4* EDS spectrum of silicon sample 12 that was generated using a graphite counter electrode that had been used for 11 prior runs. No impurities were noted.

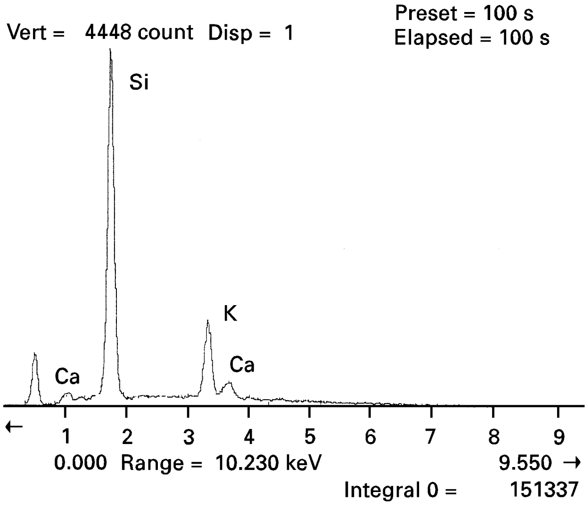

*Figure 5* EDS spectrum of silicon sample 16 that was generated with a previously unused graphite counter electrode. Impurities calcium and potassium were noted.

Deposition of the impurities continued, even with the pure ethanol, but it was observed that the amount decreased as more tests were run. Because all samples had been run using the same graphite counter electrode, it was speculated that the graphite counter electrode might be the source of the impurities. To test this hypothesis, a new graphite rod was used as a counter electrode. The EDS spectra showed that the amount of impurities increased dramatically compared to the previous samples. Fig. 4 (sample 12) shows the spectrum of a sample done after eleven runs had been performed using the same graphite counter electrode. Fig. 5 (sample 16) shows the spectrum of a sample that was generated using a previously unused graphite counter electrode. Notice the considerable difference in the amount and presence of the deposited impurities. Thus, it appears that the graphite counter electrode, when driven at high voltages, may have been the source of some of the impurities.

XPS analysis was used to examine selected deposits to identify carbon species and to confirm the presence of impurities as determined using EDS. Fig. 6 shows an XPS spectrum obtained from a carbon disc which was used as a reference material. The binding energy of the large peak, 284.3 eV, is in reasonable agreement

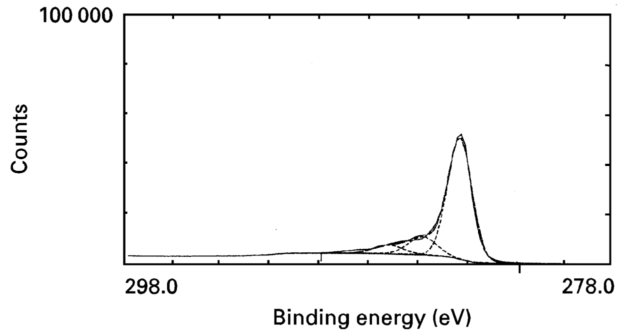

*Figure 6* XPS of the carbon disc used as a reference to detect carbon in the deposits.

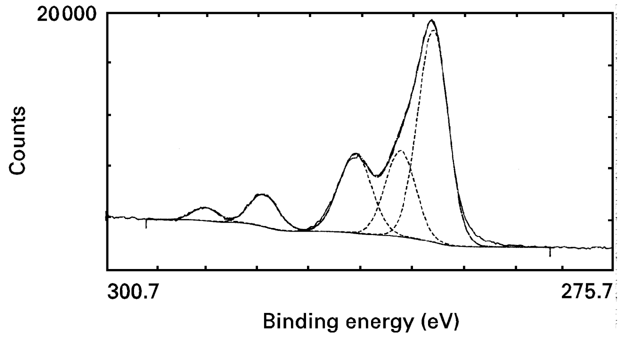

*Figure 7* XPS of sample 8 showing the presence of C–C, C–O, C=O bonding.

with literature values for C–C bonds in graphite [5, 6]. The two peaks to the higher binding-energy side of the main peak have binding energies of 285.8 and 287.2 eV. The peak at 285.8 eV is indicative of C=O [7] bonding while the peak at 287.2 eV suggests C=O bonds [7]. These latter two peaks are most likely the result of residuals from cleaning with acetone and ethanol and/or impurities from the environment.

Fig. 7 show an XPS spectrum for sample 8. The spectrum shows the presence of C–C bonds at 284.7 eV, C–O bonds at 286.3 eV [7], and C=O [7] or possibly O–C=O [8] bonds at 288.5 eV. The C–O peak and the C=O and/or O–C=O peaks account for 45% of the carbon spectrum. The peaks at 292.9 and 295.7 eV are the $2p_{3/2}$–$2p_{1/2}$ doublet for potassium. Thus, the XPS analysis using a narrow scan in the region of the C 1s peak, has shown the presence of C–C, C–O, and C=O and/or O–C=O in the deposits as well as potassium. It should be noted that XPS cannot be used unambiguously to identify diamond because diamond peaks have been reported to have binding energy values ranging from 283.5–286.2 eV depending on the surface treatment [9–11]. Therefore, as discussed below, Raman spectroscopy was used to determine if the carbon deposits had any diamond character.

XPS was also used to confirm the presence of the impurities detected on the samples by EDS. Fig. 8 shows a broad range scan of sample 16 and shows the presence of sodium, magnesium, potassium, calcium, nickel and zinc. These findings are consistent with the EDS data generated earlier. It is also notable that the intensity of the carbon and oxygen peaks are much greater than those of the deposited impurities, illustrating that the relative amounts of carbon and oxygen are higher than that of the impurities.

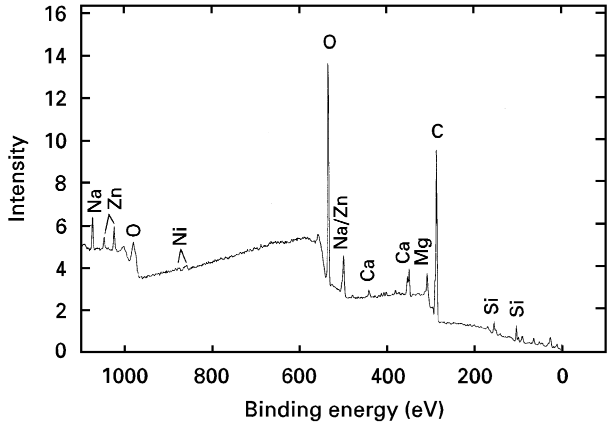

*Figure 8* XPS of sample 16 showing the large peaks indicative of carbon and oxygen, as well as the peaks indicating the impurities. sodium, zinc, calcium, magnesium and potassium. Accelerating voltage of 100 eV, step = 1.2 eV, $\mathrm{Al}K_{-\alpha}$ radiation, scan time = 33 min 22 s, 20 scans.

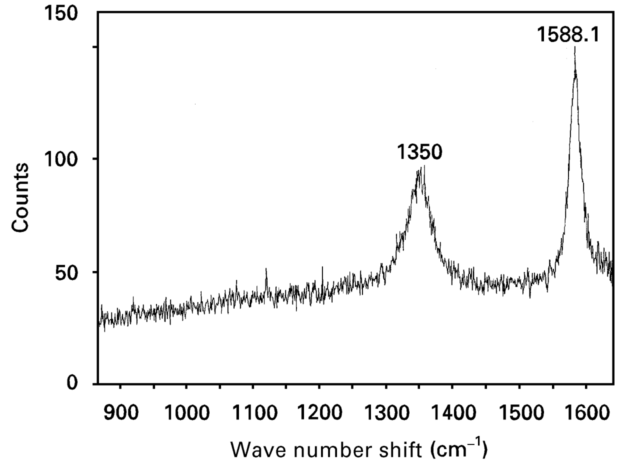

*Figure 9* Raman spectrum of sample 16, showing the peaks at 1350 and 1588.1$\mathrm{cm}^{-1}$. These peaks are indicative of amorphous carbon.

Raman spectroscopy was used to analyse several samples to determine if the carbon deposits were, in fact, diamond or diamond-like carbon. Raman is a technique that can be used to differentiate easily between diamond and other forms of carbon [12, 13]. Amorphous carbon peaks were identified on some samples, but the distinctive diamond peak at 1332 $\mathrm{cm}^{-1}$ was not observed on any of the samples. Second-order silicon peaks, due to the silicon substrate were also generated on a few samples. Fig. 9 shows the Raman spectrum from a deposit that is indicative of amorphous carbon (1350 and 1588.1 $\mathrm{cm}^{-1}$) [14]. It was also noted the samples that showed amorphous carbon peaks were the samples that had the largest amounts of impurities deposited on them. It would appear that the presence of impurities may be acting as a catalyst to the formation of amorphous carbon.

Lastly, EIS was carried out on two samples to investigate the electrical properties of the deposited film. Using Bode amplitude and phase plots, the impedance of the coated silicon was compared with the

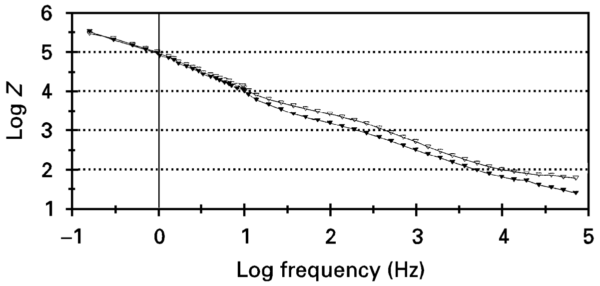

*Figure 10* Bode amplitude plot of (▼) bare and (▽) coated silicon.

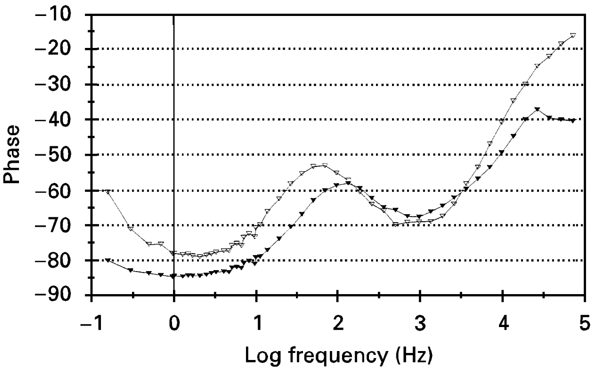

*Figure 11* Bode phase plot of (▼) bare and (▽) coated silicon.

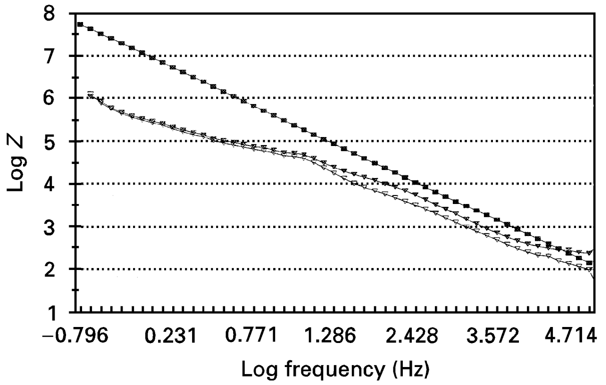

*Figure 12* Bode amplitude plot of (▽) bare and (▼) coated silicon, as compared to (■) real diamond (linear fit).

bare silicon. A Bode amplitude plot was then constructed with the capacitance of a diamond film and the impedance values of the bare and coated silicon. Figs 10 and 11 show the similarities in EIS data between the coated and bare silicon. The film does not seem to affect the electrical properties of the substrate, indicating that the film is so porous that it allows wetting of the silicon to take place. Fig. 12 compares the capacitance of the bare and coated silicon. The straight line having a slope of $-1$ represents the capacitance of a diamond film. At low frequencies, there is a large difference in the impedance of the bare and coated silicon and the diamond film. The difference becomes smaller as the frequency increaces, but not enough to match that of a diamond film.

## 4. Conclusions

1. XPS showed the presence of C–C, C–O and C=O, bonds, as well as several impurities (sodium, magnesium, potassium, calcium, nickel, zinc). Because XPS is not a precise enough method to distinguish between diamond and graphite, Raman spectroscopy was used to classify the carbon deposits further.

2. Raman spectroscopy demonstrated the presence of amorphous carbon in the films. The two broad peaks in the range 1570–1510 $\text{cm}^{-1}$ and 1390–1350 $\text{cm}^{-1}$ are indicative of the presence of amorphous carbon. Although the films are not diamond, some amorphous carbon was deposited.

3. The capacitance of the deposited film, as determined by EIS, is closer to that of the silicon substrate than to the capacitance of diamond. This is illustrated in the Bode amplitude plot, which clearly shows that at low frequencies, the capacitance of the film is very dissimilar to the capacitance of diamond. Based on this data, it seems that the film is very porous, which would result in the electrical properties of the film being comparable to that of the substrate .

4. A limited number of studies showed that the graphite rod, when used as a counter electrode and driven at high anodic voltages, released impurities into the solution. These impurities were then deposited on to the substrate. Thus, care must be taken any time graphite is used as a counter electrode at high anodic voltages. Further testing will be done to substantiate this claim.

5. Raman spectroscopy and EDS revealed that the films with the largest amounts of impurities were those identified by Raman spectroscopy as containing amorphous carbon. Deposits with low amounts of impurities only show a second-order silicon peak on the Raman spectra. It is possible that the deposited impurities are acting as a catalyst to the formation of amorphous carbon.

6. Earlier reports [1] of diamond film deposition by electrochemical means have not been substantiated. Although the same experimental procedures were followed, this work showed no evidence of diamond. The results of Raman spectroscopy showed no diamond peak, no diamond crystals were observed under SEM, and the electrochemical impedance spectroscopy reported a capacitance of the deposited film that was very different from that of real diamond.

## Acknowledgement

We acknowledge the USNA-NRL Cooperative Research Program for its assistance. In addition, we thank Pehr Pehrsson and Terri McCormick, Naval Research Laboratory, for help with the Raman spectroscopy, Dr. John Murray for assistance with the EIS study, and John Hein for sample preparation.

## References

1. Y. NAMBA, *J. Vac. Sci Technol. A* **10** (1992) 3368.
2. T. SUZUKI, Y.MANITA, T. YAMAZAKI, S. WADA, and T. NOMA, *J. Mater, Sci.* **30** (1995) 2067.

3. M. J. SHANE, B. K. CHINH, and M. J. SAILOR, "Extended Abstracts," Electrochemical Society, Fall Meeting, Chicago, IL, 8-13, October 1995.
4. A. H. DEUTCHMANN, R. J. PARTYKA, *Adv. Mater. Proc.* June (1989) 29.
5. J. F. MOULDER, W. F. STICKLE, P. E. SOBOL and K. D. BOMBEN, "Handbook of X-ray Photoelectron Spectroscopy" (Perkin–Elmer, Eden Prairie, MN, 1992) p. 225.
6. C. D. WAGNER, in "Practical Surface Analysis", Vol. 1, 2nd Edn, edited by D. Briggs and M. P. Seah (Wiley New York, NY, 1990) Appendix 5.
7. D. BRIGGS, *ibid.*, Ch. 9.
8. G. P. LOPEZ, D. G. CASTNER and B. D. RATNER, *Surf. Interface Anal.* **17** (1991) 267.
9. R. G. CAVELL, S. P. KOWALCZYK, L. LEY, R. A. POLLAK, B. MILLS, D. A SHIRLEY and W. PERRY, *Phys. Rev. B* **7** (1973) 5313.
10. P. E. PEHRSSON, in "Proceedings of the Third International Symposium on Diamond Materials", edited by J. P. Dismukes, K. V. Ravi, B. Lux and N. Setaka, (The Electrochemical Society, Pennington, NJ, 1993) p. 668.
11. R. GRAUPER, J. RISTEIN, and L. LEY, *Surf. Sci.* **320**, (1994) 201.
12. D. E. NEWBURY, D. C. JOY, P. ECHLIN, C. E. FIORI and J. I. GOLDSTEIN, "Advanced Scanning Electron Microscopy and X-Ray Microanalysis" (Plenum Press, New York 1986) p. 289.
13. D. S. KNIGHT, and W. B. WHITE, *J. Mater. Res.* **4** (2) (1989) 385.
14. M. YOSHIKAWA, G. KATAGIRI, H. ISHIDA, A. ISHITANI and T. AKAMATSU, *Appl. Phys. Lett.* **52** (1988) 1639.

*Received 23 August*
*and accepted 30 October 1996*